

# Optical binding of particles with or without the presence of a flat dielectric surface

P. C. Chaumet and M. Nieto-Vesperinas

*Instituto de Ciencia de Materiales de Madrid, Consejo Superior de Investigaciones Científicas,  
Campus de Cantoblanco Madrid 28049, Spain*

(Received 29 November 2000; published 28 June 2001)

Optical fields can induce forces between microscopic objects, thus giving rise to different structures of matter. We study theoretically these optical forces between two spheres, either isolated in water, or in the presence of a flat dielectric surface. We observe different behavior in the binding force between particles at large and at small distances (in comparison with the wavelength) from each other. This is due to the great contribution of evanescent waves at short distances. We analyze how the optical binding depends on the size of the particles, the material composing them, the wavelength, and, above all, the polarization of the incident beam. We also show that depending on the polarization the force between small particles at small distances changes its sign. Finally, the presence of a substrate surface is analyzed, showing that it only slightly changes the magnitudes of the forces, but not their qualitative nature, except when one employs total internal reflection, in which case the particles are induced to move together along the surface.

DOI: 10.1103/PhysRevB.64.035422

PACS number(s): 78.70.-g, 03.50.De, 42.50.Vk

## I. INTRODUCTION

Some time ago, it was demonstrated that optical fields can produce forces on neutral particles;<sup>1,2</sup> since then this mechanical action has been used in optical tweezers<sup>3</sup> and more recently in optical force microscopy,<sup>4,5</sup> as well as in manipulating molecules<sup>6</sup> and dielectric spheres.<sup>7-9</sup> In addition, the possibility of binding objects<sup>10</sup> through optical forces and thus creating microstructures, in on- or off-resonant conditions,<sup>11-13</sup> was pointed out.

In this paper we wish to undertake a detailed study of optical forces on neutral particles, based on a rigorous analysis that we have carried out<sup>14-16</sup> in a full three-dimensional configuration by using the coupled dipole method of Purcell and Pennypacker<sup>17</sup> via the Maxwell stress tensor.<sup>18</sup> Specifically, we study the forces induced by light between two spheres, either isolated in solution, or in the presence of a flat dielectric surface. We shall monitor the nature, either attractive or repulsive, of the light induced force between the spheres, according to the wavelength, polarization of the incident wave, and size and composition of the spheres.

In Sec. II we outline the calculation method employed to determine the optical binding forces; then, in Sec. III we present results for spheres either isolated in water (Sec. III A) or suspended in this liquid in the presence of a flat dielectric interface (Sec. III B).

## II. METHOD USED FOR COMPUTING THE OPTICAL BINDING

In a previous article<sup>14</sup> we showed the possibility of computing the optical forces on a sphere with the coupled dipole method.<sup>17</sup> For the computation of the optical binding between particles, we now use the same procedure; thus we shall only outline the main equations and the changes introduced in them to address the presence of multiple objects.

Let  $K$  objects be above a flat dielectric surface. Each object is discretized into  $N_k$  subunits, with  $k=1, \dots, K$ . Following the procedure of Ref. 17, the field at the  $(i,k)$ th sub-

unit, namely, the  $i$ th subunit of the  $k$ th object, can be written as

$$\mathbf{E}(\mathbf{r}_i^k, \omega) = \mathbf{E}_0(\mathbf{r}_i^k, \omega) + \sum_{l=1}^K \sum_{j=1}^{N_l} [\mathbf{S}(\mathbf{r}_i^k, \mathbf{r}_j^l, \omega) + \mathbf{T}(\mathbf{r}_i^k, \mathbf{r}_j^l, \omega)] \alpha_j^l \mathbf{E}(\mathbf{r}_j^l, \omega), \quad (1)$$

where  $\alpha_j^l$  is the polarizability of the  $(j,l)$  subunit,  $\mathbf{T}$  is the linear response to a dipole in free space,<sup>19</sup> and  $\mathbf{S}$  represents the linear response of a dipole in the presence of a surface.<sup>20,21</sup> The value of the electric field at each subunit position is obtained by solving the linear system Eq. (1) written for all subunits, so that the size of the system to solve is  $\prod_{k=1}^K N_k$ . Once the electric field is obtained, the component of the total averaged force on the  $(i,k)$ th subunit can be deduced from both the field and its derivative at its position  $\mathbf{r}_i^k$ :<sup>15</sup>

$$F_u(\mathbf{r}_i^k) = (1/2) \text{Re} \sum_{v=1}^3 \left( p_v(\mathbf{r}_i^k, \omega) \frac{\partial E_v^*(\mathbf{r}_i^k, \omega)}{\partial u} \right) \quad (u=1,2,3), \quad (2)$$

where  $u, v$  stand for  $x, y, z$ , and  $\mathbf{p}(\mathbf{r}_i^k, \omega)$  is the electric dipole of the  $(i,k)$ th subunit due to the incident field and all the other subunits. Note that the derivative of the field can be obtained from the derivative of Eq. (1).<sup>14</sup> Then the following relation can be written:

$$\mathbf{F}^k = \sum_{i=1}^{N_k} \mathbf{F}(\mathbf{r}_i^k), \quad (3)$$

where  $\mathbf{F}^k$  is the total force on the  $k$ th object due to both the incident field and the multiple interaction with the surface and the other  $K-1$  objects. If the  $k$ th object is a sphere small compared to the wavelength, the dipole approximation can be made; hence  $N_k=1$ . We also remark that, in what follows, when we represent the normalized force, this means  $\mathbf{F}/(4\pi\epsilon_0|\mathbf{E}_i|^2)$ , where  $\epsilon_0$  is the permittivity of vacuum and  $|\mathbf{E}_i|^2$  denotes the intensity of the incident beam.

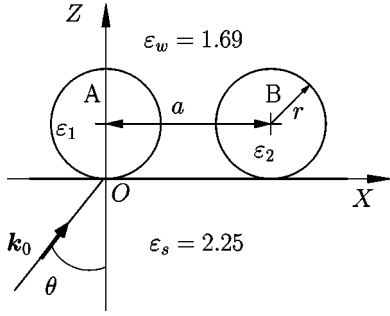


FIG. 1. The most complex geometry considered in this paper: two spheres of radius  $r$  on a dielectric flat surface. The spheres are embedded in water with  $\varepsilon_w = 1.69$ , and the relative permittivity of the surface is  $\varepsilon_s = 2.25$ . The incident wave vector  $\mathbf{k}_0$  is in the  $XZ$  plane, and  $\theta$  is the angle of incidence.

### III. RESULTS AND DISCUSSION

In Fig. 1 we represent the more complex geometry that we shall consider in this work. Two spheres (either dielectric or metallic) are embedded in water ( $\varepsilon_w = 1.69$ ). Illumination with an incident plane wave takes place in the  $XZ$  plane at an angle of incidence  $\theta$ . When a dielectric flat surface at  $z=0$  is used, we consider it separating glass ( $\varepsilon_s = 2.25$ ) at  $z < 0$  from water ( $z > 0$ ).

#### A. Particles in water

In this section we do not address yet the presence of the surface ( $\varepsilon_s = \varepsilon_w = 1.69$ ), i.e.,  $\mathbf{S}(\mathbf{r}_i^k, \mathbf{r}_j^l, \omega) = 0$  in Eq. (1), and the angle of incidence is  $\theta = 0^\circ$ . Even in the absence of a surface, we make reference to the polarization and thus we shall always use the terms  $p$  polarization and  $s$  polarization when the electric field vector is in the  $XZ$  plane and along the  $Y$  axis, respectively.

We begin with the simplest case, i.e., the radius  $r$  of the two particles is small compared to the wavelength employed. As previously said, we then use the dipole approximation. We study, first, the case of two identical spheres with  $\varepsilon_1 = \varepsilon_2 = 2.25$  and radius  $r = 10$  nm at a wavelength  $\lambda = 632.8$  nm in vacuum. Figure 2 represents the force along the  $X$  direction on the sphere  $B$  at different positions of this sphere on the  $X$  axis. The sphere  $A$  remains fixed. We have plotted only the force exerted on sphere  $B$ , since by symmetry the force along the  $X$  axis on sphere  $A$  is opposite to that on  $B$ . We observe two facts: first, the oscillation of the force when the spheres are far from each other, and, second, the strong force, either attractive or repulsive, when the spheres are very close to each other, depending on the polarization. For a better understanding of the physical process, using Eq. (1) and its derivative for two dipolar objects, we can analytically determine, through Eq. (2), the force on the spheres. Then, on using the fact that there is a plane wave in the  $Z$  direction (the incident wave is  $E_0 e^{ik_0 z}$ , where  $i = x$  or  $y$  depending on the polarization of the incident field) the force on the second sphere can be written as

$$F_x(\mathbf{r}_2) = \frac{1}{2} \text{Re} \left( \alpha_2 E_i(\mathbf{r}_2, \omega) \alpha_1^* E_i^*(\mathbf{r}_1, \omega) \frac{\partial}{\partial x} T_{ii}^*(\mathbf{r}_2, \mathbf{r}_1, \omega) \right), \quad (4)$$

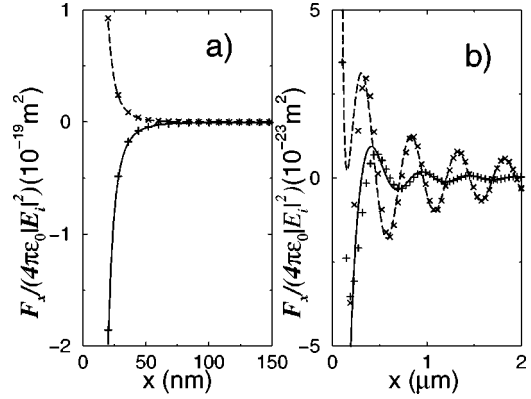


FIG. 2. Normalized force in the  $X$  direction on sphere  $B$  versus distance  $x$  between the centers of the spheres. Both spheres are of glass ( $\varepsilon_1 = \varepsilon_2 = 2.25$ ), with  $r = 10$  nm. The angle of incidence of the illuminating plane wave is  $\theta = 0^\circ$  and the wavelength  $\lambda = 632.8$  nm in vacuum. The full line corresponds to  $p$  polarization, and the dashed line represents  $s$  polarization. (a) Force for short distances between the spheres; the symbols  $+$  ( $\times$ ) correspond to the values from the nonretarded approximation for  $p$  polarization ( $s$  polarization). (b) Force in far field; the symbols  $+$  ( $\times$ ) represent the values from the nonretarded approximation in far field for  $p$  polarization ( $s$  polarization).

where  $i = x$  for  $p$  polarization and  $i = y$  for  $s$  polarization of the incident field. Notice that to obtain the force on sphere  $A$  the indices 1 and 2 must be permuted. But, even in this simple case, the exact analytical solution of Eq. (4) is not easy to interpret. Hence, we make in Eq. (1) the approximation that the term  $\mathbf{T}(\mathbf{r}_i^k, \mathbf{r}_j^l, \omega) \alpha_j^l$  is smaller than 1 (we will discuss this approximation further). Now, if we use the hypothesis that the two spheres are identical ( $\alpha_1 = \alpha_2$ ), Eq. (4) becomes

$$F_x(\mathbf{r}_2) = \frac{1}{2} |\alpha_1 E_{0i}|^2 \text{Re} \left( \frac{\partial}{\partial x} T_{ii}(\mathbf{r}_2, \mathbf{r}_1, \omega) \right). \quad (5)$$

At short distances we can make the nonretarded approximation ( $k_0 = 0$ ) and, as shown in the Appendix, we have that  $F_x(\mathbf{r}_2) = -3 |\alpha_1 E_{0x}|^2 / a^4$  in  $p$  polarization and  $F_x(\mathbf{r}_2) = (3/2) |\alpha_1 E_{0y}|^2 / a^4$  in  $s$  polarization. The points (with the symbols  $+$  and  $\times$ ) obtained with this approximation are shown in Fig. 2(a) and fit the curves obtained correctly without any approximation, as seen in this figure. Thus, they validate the approximation  $\mathbf{T}(\mathbf{r}_i^k, \mathbf{r}_j^l, \omega) \alpha_j^l \ll 1$  previously made. Only when the spheres are very close to each other does this approximation slightly depart from the exact calculation due to the increase of the free space susceptibility. In fact, this approximation assumes the dipole associated with the spheres to be due only to the incident field, which is a good assumption when the polarizabilities are small, as for glass spheres. It is now easy to physically understand from Eq. (5) the reason for this either attractive or repulsive force. As the spheres are small, the scattering force is negligible<sup>22</sup> and thus only the gradient force remains, due to the interaction between the dipole associated with sphere  $B$ , and to the variation of the field created by sphere  $A$  at the position of

sphere  $B$ . In  $p$  polarization, the field due to sphere  $A$  at the position of sphere  $B$  and the dipole of sphere  $B$  are in phase; hence sphere  $B$  is pushed to the higher intensity region, namely, toward sphere  $A$ . In  $s$  polarization, as the field due to sphere  $A$  at the position of sphere  $B$  and the dipole of sphere  $B$  are in opposite phase, sphere  $B$  is pushed to the lower intensity region, namely, far from sphere  $A$ . One can observe a similar effect in an atom mirror,<sup>23</sup> or on a small silver particle in an evanescent field.<sup>16</sup>

On the other hand, in the far field we obtain, from the Appendix, the force upon sphere  $B$  as  $F_x(\mathbf{r}_2) = |\alpha_1 E_{0x}|^2 k_0^2 \cos(k_0 a)/a^2$  in  $p$  polarization and  $F_x(\mathbf{r}_2) = -|\alpha_1 E_{0x}|^2 k_0^3 \sin(k_0 a)/(2a)$  in  $s$  polarization, with  $k_0 = 2\pi\sqrt{\epsilon_w}/\lambda$ . The same explanation as before can be used for the sign of the force: following the phase relationship between the dipole and the field due to sphere  $A$ , the force is either positive or negative; hence, the oscillations of the force  $F_x$  take place with period  $\lambda/\sqrt{\epsilon_w}$ . The phase difference  $\lambda/(4\sqrt{\epsilon_w})$  that appears in the far field between the oscillations of  $s$  and  $p$  polarization comes from the difference between the derivatives of the components  $xx$  and  $yy$  of the free space susceptibility. We observe that the force in  $p$  polarization decreases faster than in  $s$  polarization; this is due to the absence of a propagating field along the  $X$  axis in the far field. The magnitude of the force differs by a factor of  $10^4$  between far field and near field. This is due to the strong interaction between the spheres through the evanescent waves.

We can make an analogy in the near field with molecular physics. If we look at the dipole moments of the two spheres, we compare our system of forces with the interaction between two molecules. In  $p$  polarization, as the dipole moments are aligned and antisymmetric, they produce an attractive force analogous to that between two orbitals  $p_z$ , giving rise to a bonding state  $\sigma_u$ . In  $s$  polarization, the dipole moments are parallel and symmetric, so we have antibonding states  $\pi_g^*$ , where  $*$  means that the two spheres cannot be bound.

We represent in Fig. 3 the force along the  $Z$  direction. In this case the scattering force is predominant. The interaction between the spheres is now directly responsible for the oscillation of the force. Notice that when the spheres are far from each other, as the interaction between the spheres becomes weak when the distance increases, the force tends toward the scattering force upon one sphere due to the incident field. As this force is not responsible for optical binding, we are not going to discuss it further.

More interesting is the case of two different small spheres, one ( $B$ ) being dielectric and the other ( $A$ ) being metallic (silver). The first fact easily observed from Eq. (4) pertains to the nonretarded case; as the derivative of the free space susceptibility is real, the forces on spheres  $A$  and  $B$  are equal but of opposite sign to each other (this is no longer the case in the far field). In Fig. 4 we represent the force on sphere  $B$  at short distances from sphere  $A$  (in comparison with the wavelength), for  $\lambda = 365$  nm, 388.5 nm, and 600 nm. For  $p$  polarization, we observe that the force at the wavelength  $\lambda = 365$  nm has a rather strange behavior as it is

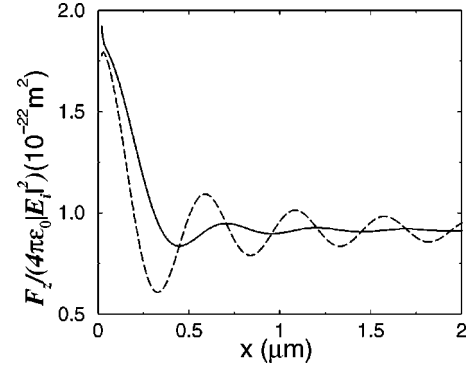


FIG. 3. Normalized force in the  $Z$  direction on sphere  $B$  versus distance  $x$  between the centers of the spheres. Both spheres are of glass with  $r = 10$  nm,  $\theta = 0^\circ$ , and  $\lambda = 632.8$  nm in vacuum. The full line corresponds to  $p$  polarization, whereas the dashed line represents  $s$  polarization.

positive, and only when the spheres are almost in contact does this force change and become similar to those at the other wavelengths. With the approximation  $\mathbf{T}(\mathbf{r}_i^k, \mathbf{r}_j^l, \omega) \alpha_j^l \ll 1$ , the force in the nonretarded approximation can be written

$$F_x(\mathbf{r}_2) = 1/2 \frac{\partial T_{ii}(\mathbf{r}_2, \mathbf{r}_1, \omega)}{\partial x} |E_0|^2 \alpha_2 \text{Re}(\alpha_1). \quad (6)$$

We observe that the sign of the force depends on  $\text{Re}(\alpha_1)$ . When  $\text{Re}(\alpha_1) > 0$  ( $\lambda = 600$  nm), which is the common case, the dipole associated with the silver sphere is in phase with the applied field, so everything happens as for the dielectric sphere. Conversely, when  $\text{Re}(\alpha_1) < 0$  ( $\lambda = 365$  nm) the dipole is in opposite phase to the applied field, and hence the force becomes positive. But when the spheres are almost in contact the approximation  $\mathbf{T}(\mathbf{r}_i^k, \mathbf{r}_j^l, \omega) \alpha_j^l \ll 1$  is no longer valid as shown when  $\text{Re}(\alpha_1) = 0$  ( $\lambda = 388.5$  nm), in which case the force is not null but negative. This is due to the fact that the polarizability of the silver sphere is large and hence the approximation is no longer valid for short distances. Physically, this represents the contribution of the metallic

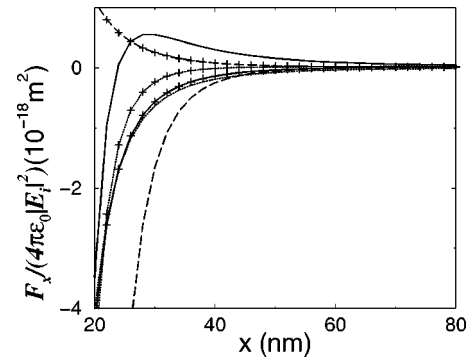


FIG. 4. Nonretarded approximation normalized force in the  $X$  direction on sphere  $B$  versus distance  $x$  between the centers of the spheres. The sphere  $A$  is of silver and the sphere  $B$  is of glass with  $r = 10$  nm.  $\lambda = 365$  nm (full line), 388.5 nm (dotted line), and 600 nm (dashed line). Without symbols,  $p$  polarization; with symbol  $+$ ,  $s$  polarization.

sphere to the electric field acting on the dielectric sphere, which is larger than that of the incident field; hence the dipoles associated with the two spheres are in phase and the force is attractive. Notice that the change of sign occurs both at the plasmon resonance [ $\text{Re}(\epsilon_1) \approx -2\epsilon_w$ ] and when  $\text{Re}(\epsilon_1) \approx \epsilon_w$ . When  $\epsilon_1$  is between these two values, the real part of the polarizability is negative. For a more complete discussion of this, one can see Ref. 16. Similar reasoning applies for  $s$  polarization. If we now make the analogy previously done with the molecular orbitals, then depending on the wavelength in  $s$  polarization we shall obtain either anti-bonding states  $\pi_g^*$  or bonding states  $\pi_u$ .

In the far field, for  $p$  polarization, on using Eq. (4) and the approximation  $\mathbf{T}(\mathbf{r}_i^k, \mathbf{r}_j^l, \omega) \alpha_j^l \ll 1$ , we can write the force on the sphere  $B$  as

$$F_x(\mathbf{r}_2) = [\text{Re}(\alpha_1^* \alpha_2) \cos(k_0 a) - \text{Im}(\alpha_1^* \alpha_2) \sin(k_0 a)] k_0^2 |E_{0x}|^2 / a^2 \quad (7)$$

and the force on sphere  $A$  as

$$F_x(\mathbf{r}_1) = [-\text{Re}(\alpha_1^* \alpha_2) \cos(k_0 a) - \text{Im}(\alpha_1^* \alpha_2) \sin(k_0 a)] k_0^2 |E_{0x}|^2 / a^2. \quad (8)$$

As the spheres are small, we can take only the gradient force as this is now the predominant one; then  $\alpha_2$  is real.<sup>15</sup> Therefore, the forces on spheres  $A$  and  $B$  for the wavelength  $\lambda = 600$  nm, where  $\text{Im}(\alpha_1)$  is weak, are opposite to each other as for two identical spheres. But at  $\lambda = 388.5$  nm, where  $\text{Re}(\alpha_1) = 0$ , the forces on the two spheres are completely identical.

It should be remarked that, if the laser intensity of the incident light is assumed to be  $0.2 \text{ W}/\mu\text{m}^2$ ,<sup>24</sup> the optical forces for these small spheres are not strong enough to create optical binding, since then the Brownian motion remains the dominant force. In this respect, the interest of the case of these small spheres is mainly the interpretative value it yields for the underlying physics. However, for larger radius in comparison to the wavelength, the forces become larger and so does the trapping potential. In Figs. 5(b) and 6(b) we plot the force along the  $X$  axis for two dielectric spheres (glass) with radius  $r = 100$  nm and  $200$  nm, respectively. We observe that with the intensity used previously ( $0.2 \text{ W}/\mu\text{m}^2$ ) the magnitude of the force is now enough to optically bind both spheres. We compute the potential energy of the optical trap by integration of the force (we take the potential energy as null when the second sphere is at infinity). As the two spheres are identical, the potential energy is the same for both. The efficiency of the trapping force requires it to be larger than the force due to the Brownian motion; hence the depth of the potential wells of the trap should be larger than  $k_b T$ ,  $T$  being the temperature of water and  $k_b$  the Boltzmann constant. Considering  $T = 290$  K, then  $k_b T = 4 \times 10^{-21}$  J. We plot in Figs. 5(a) and 6(a) the potential normalized to the value  $k_b T$ . We adopt the criterion that the trap is efficient when the potential well is larger than  $3k_b T$ . Hence the bars plotted at the bottom of the wells in Figs. 5(a) and 6(a) correspond to the value 3. We see from Fig. 5 that for  $p$

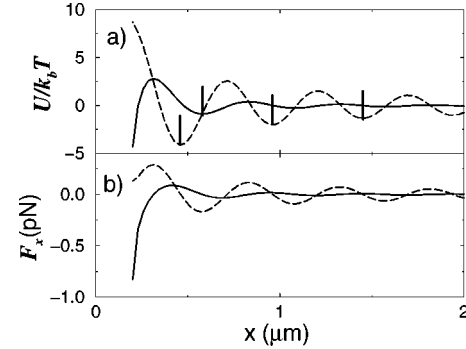


FIG. 5. Two glass spheres of radius  $r = 100$  nm,  $\theta = 0^\circ$ , and  $\lambda = 632.8$  nm in vacuum. The laser intensity of the incident light is  $0.2 \text{ W}/\mu\text{m}^2$ . Full line curves are for  $p$  polarization. Dashed line curves correspond to  $s$ -polarization. (a) Potential of sphere  $B$  normalized to  $k_b T$  versus distance between the centers of the spheres. The height of the bars corresponds to a normalized potential equal to 3. (b) Force in the  $X$  direction versus the distance between the spheres.

polarization the trap is not feasible except when the spheres are in contact. For  $s$  polarization, we have three equilibrium positions spaced out by one wavelength. This behavior is explained by the previous results on small spheres, and in agreement with experiments.<sup>10</sup> When the size of the sphere is close to one wavelength, we see from Fig. 6 that the depth of the potential well is larger than in the previous case. In  $p$  polarization there is no possibility of sticking the spheres together, but now we have one potential minimum of stable position. Thus, we observe that it is easier to trap particles when their radii are large, in agreement with the experiments of Burns *et al.*<sup>10</sup>

Notice that the gravity force is  $6.16 \times 10^{-5}$  pN and  $4.93 \times 10^{-4}$  pN for the spheres of radii  $r = 100$  nm and  $200$  nm, respectively. Another force that exists between the spheres is the Casimir-Polder force  $F_c$ . To our knowledge,  $F_c$  has often been studied either between two plates or between a sphere and a plate,<sup>25</sup> but it has never been established between two spheres. In the nonretarded approximation and the dipole approximation for the spheres,  $F_c$  is reduced to the dispersion force (London's force) which is inversely proportional to the seventh power of the distance between the dipoles (see, for example, Ref. 26). Hence, only when the spheres are in contact, or at distances smaller than

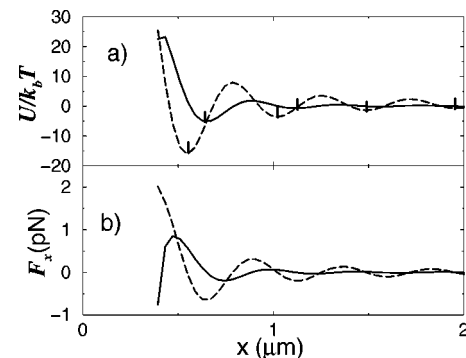


FIG. 6. Same as Fig. 5 but with a radius  $r = 200$  nm.

TABLE I. Minimum radius in nm to get one minimum position of the potential for two identical spheres. The following cases are addressed: glass sphere and silver sphere (both off and on plasmon resonance). The criterion of stability used is that the potential well depth must be larger than  $3k_bT$ .

Spheres	Glass ( $\lambda = 632.8$ nm)	Silver ( $\lambda = 394$ nm)	Silver ( $\lambda = 314$ nm)
Limiting radius in nm ( $p$ pol.)	123	33	180
Limiting radius in nm ( $s$ pol.)	85	21	50

the wavelength from each other, might this force be of the same magnitude as the optical forces. However, the fast decay of this force at distances larger than the wavelength prevents it from perturbing the optical trap.

In Table I we give some examples of the limiting radius to get optical trapping for two identical spheres embedded in water (notice that for  $p$  polarization we do not mean optical trapping when the spheres are stuck in contact), i.e., the minimum radius to obtain one potential minimum or stable position for the two spheres using the same criterion as before (namely,  $U > 3k_bT$ ). We should remark that this is the limiting radius only to obtain the first stable position; if we want to get more stable positions, as in Ref. 10, the radius must be larger. As mentioned before, the table shows that the optical trapping is easier for  $s$  polarization. For the silver sphere, the value  $\lambda = 394$  nm corresponds to the plasmon resonance, and that of  $\lambda = 314$  nm is for a wavelength out of resonance. At the plasmon resonance the polarizability is largest, so it is easier to perform optical binding at this wavelength.

As a last instance, we now consider two spheres in free space, with radii  $r = 100$  nm, one being of glass and the other of silver, illuminated by a plane wave at  $\lambda = 388.5$  nm. We plot in Fig. 7 the potential energy for the two polarizations and the two spheres, since now this magnitude depends on the sphere material. We then observe that it is not possible to obtain a stable equilibrium since the potentials of the two spheres are now different. This result is explainable from the previous calculation on small spheres (of silver and glass),

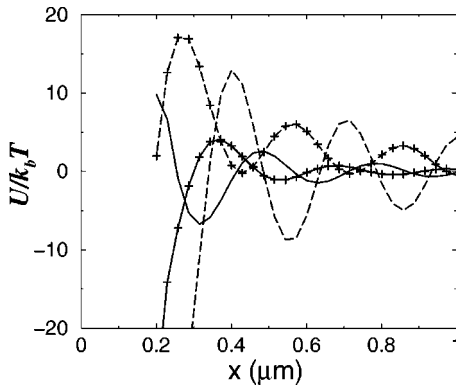


FIG. 7. The sphere  $A$  is of glass and the sphere  $B$  of silver with  $r = 100$  nm,  $\lambda = 388.5$  nm. The laser intensity of the incident light is  $0.2 \text{ W}/\mu\text{m}^2$ . Plot of the potential normalized to  $k_bT$  for the two spheres versus the distance between them. The full line is for  $p$  polarization and dashed line corresponds to  $s$  polarization. The potential of sphere  $A$  is without symbols, and the potential of sphere  $B$  is with symbol  $+$ .

since then the forces were always opposed to each other at this wavelength. In fact, as the spheres are now large, the forces at this wavelength are not exactly in opposition, due to the larger scattering and absorbing force. Hence it is possible to obtain points where the potential of the two spheres is minimum. This happens when the forces on each sphere are the same and positive. In that case, the two spheres move in the direction of the positive  $X$  axis while keeping constant the distance between them.

### B. Particles in water on a dielectric flat surface

In this section we consider a flat dielectric surface upon which the spheres are suspended in water, as shown by Fig. 1. We compute the force along the  $X$  axis on sphere  $B$  when both spheres are dielectric (glass), with  $\theta = 0^\circ$  (Fig. 8). We now observe that for both large and small spheres the force has a behavior similar to that acting on dielectric spheres isolated in water. When the spheres are in contact, the force on sphere  $B$  is the same as in the absence of the interface, whereas when the spheres are far from each other this force is slightly smaller than that without the interface. This means that optical binding is more difficult to perform when the spheres are on a surface than when they are far from interfaces. Also, there is a change in the period of oscillation due to interaction between the spheres via the light reflected by the surface. However, in the case when one of the spheres is metallic (silver), we observe the same behavior of the forces when the surface is present as without it. Thus, as previously observed for dielectric spheres, there appears only a shift in the oscillation and magnitude of the forces.

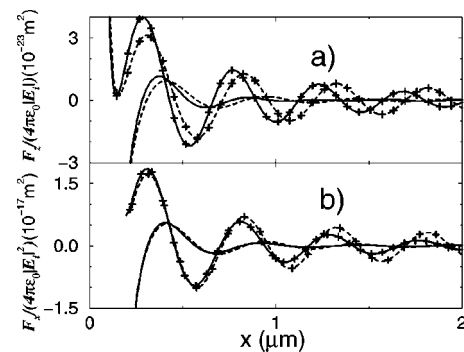


FIG. 8. Force in the  $X$  direction upon sphere  $B$  when the spheres are placed on a flat dielectric surface.  $\theta = 0^\circ$ ,  $\lambda = 632.8$  nm. The full line represents the force in the presence of the surface, and the dashed line corresponds to the force computed without the interface. The curves with symbols  $+$  denote  $s$  polarization, and those without symbols correspond to  $p$  polarization. (a) Spheres of glass with  $r = 10$  nm. (b) Spheres of glass with  $r = 100$  nm.

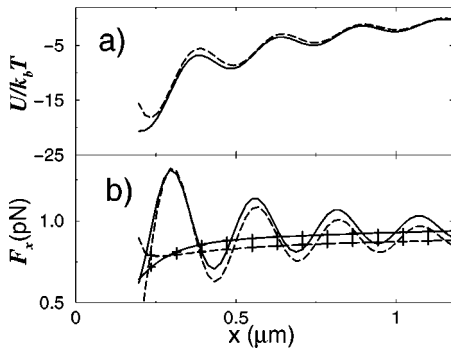


FIG. 9. Two glass spheres of radius  $r=100$  nm in vacuum, in front of a flat dielectric surface.  $\theta=50^\circ$ ,  $\lambda=632.8$  nm. The laser intensity of the incident light is  $0.2 \text{ W}/\mu\text{m}^2$ . Full line curves are for  $p$  polarization. Dashed line curves correspond to  $s$  polarization. (a) Potential of interaction between the two spheres, normalized to  $k_b T$ , versus distance between the centers of the spheres. (b) Force in the  $X$  direction against distance between the spheres. The curve of force on sphere  $A$  is without symbols, and the force on sphere  $B$  is marked with symbol  $+$ .

In Fig. 9 we investigate the potential and optical force on two glass spheres in front of a dielectric surface, illuminated by total internal reflection ( $\theta=50^\circ$ ). Figure 9(b) shows that the force component along the  $X$  axis always pushes the spheres in the direction of the wave vector component parallel to the surface. Hence, it is not possible to obtain a stable equilibrium with the two spheres remaining fixed. But if we compute the potential of the two spheres together [Fig. 9(a)], we observe some minima, indicating that the system can acquire internal equilibrium, namely, the relative positions of the spheres can be kept fixed. Hence, when both spheres move impelled by the evanescent wave propagating along the surface, their velocity remains parallel to this surface, while the distance between them keeps some particular values given by the positions of the potential minima [cf. Fig. 9(a)]. Notice that the force on the second sphere (in both polarizations) has no oscillation; a very similar behavior was observed by Okamoto and Kawata.<sup>24</sup> The computational prediction of similar collective movements in systems of more than two spheres will involve long computing times of their relative positions by potential energy minimization.

#### IV. CONCLUSION

We have studied the optical binding between two spheres embedded in water, in either the presence or absence of a flat dielectric interface. We have presented results for different sizes and illumination conditions. Some of them agree with

previous experiments<sup>10</sup> for two identical spheres; however, when they are composed of different materials, the force between them may have quite different behavior, depending on the wavelength of the light employed. In future work, it would be interesting to investigate the effect of light on several spheres in water in order to build up particle arrays. However, the vertical force that pushes the spheres away from the substrate constitutes a hindrance to this aim. This work shows, however, that this problem can be avoided by illuminating the system under total internal reflection at the substrate interface. Then the spheres will be stuck to the surface by the gradient force due to the transmitted evanescent wave. The horizontal force of this surface wave on the sphere, which pushes them along the interface, can be compensated by means of a second counterpropagating evanescent wave, created by an additional beam. Notice, in addition, that if both surface waves are mutually coherent, the resulting standing wave pattern can introduce further structure in the resulting potential wells seen by the spheres.

#### ACKNOWLEDGMENTS

This work was supported by the European Union and the Direccion General de Investigacion Cientifica y Tecnica, Grant No. PB98 0464.

#### APPENDIX: DERIVATIVE OF THE FREE SPACE SUSCEPTIBILITY

The derivative of the free space susceptibility used in this paper is

$$\frac{\partial}{\partial x} T_{xx}(x, x_0) = -\frac{6\mathbf{a}}{a^5}, \quad (\text{A1})$$

$$\frac{\partial}{\partial x} T_{yy}(x, x_0) = \frac{\partial}{\partial x} T_{zz}(x, x_0) = \frac{3\mathbf{a}}{a^5} \quad (\text{A2})$$

in the nonretarded case, and

$$\frac{\partial}{\partial x} T_{xx}(x, x_0, \omega) = \frac{2\mathbf{a}k_0^2}{a^3} e^{ik_0 a}, \quad (\text{A3})$$

$$\frac{\partial}{\partial x} T_{yy}(x, x_0, \omega) = \frac{\partial}{\partial x} T_{zz}(x, x_0, \omega) = \frac{i\mathbf{a}k_0^3}{a^2} e^{ik_0 a} \quad (\text{A4})$$

in the far field, where  $\mathbf{a}=(x-x_0)$  and  $a=|\mathbf{a}|$ .  $x$  is the abscissa of the observation point and  $x_0$  that of the dipole position.

<sup>1</sup>A. Ashkin, Phys. Rev. Lett. **24**, 156 (1970).

<sup>2</sup>A. Ashkin, Phys. Rev. Lett. **25**, 1321 (1970).

<sup>3</sup>A. Ashkin, J. M. Dziedzic, J. E. Bjorkholm, and S. Chu, Opt. Lett. **11**, 288 (1986).

<sup>4</sup>A. R. Clapp, A. G. Ruta, and R. B. Dickinson, Rev. Sci. Instrum.

**70**, 2627 (1999).

<sup>5</sup>A. C. Dogarin and R. Rajagopalan, Langmuir **16**, 2770 (2000).

<sup>6</sup>A. Ashkin and J. M. Dziedzic, Science **235**, 1517 (1987).

<sup>7</sup>S. D. Collins, R. J. Baskin, and D. G. Howitt, Appl. Opt. **38**, 6068 (1999).

- <sup>8</sup>R. C. Gauthier and A. Frangioudakis, *Appl. Opt.* **39**, 26 (2000).
- <sup>9</sup>K. Taguchi, K. Atsuta, T. Nakata, and M. Ikeda, *Opt. Commun.* **176**, 43 (2000).
- <sup>10</sup>M. Burns, J.-M. Fournier, and J. Golovchenko, *Phys. Rev. Lett.* **63**, 1233 (1989).
- <sup>11</sup>M. I. Antonoyiannakis and J. B. Pendry, *Phys. Rev. B* **60**, 2363 (1999).
- <sup>12</sup>M. I. Antonoyiannakis and J. B. Pendry, *Europhys. Lett.* **40**, 613 (1997).
- <sup>13</sup>M. Bayer, T. Gutbrod, A. Forchel, T. L. Reinecke, P. A. Knipp, A. A. Dremin, V. D. Kulakovskii, and J. P. Reithmaier, *Phys. Rev. Lett.* **81**, 2582 (1997).
- <sup>14</sup>P. C. Chaumet and M. Nieto-Vesperinas, *Phys. Rev. B* **61**, 14 119 (2000).
- <sup>15</sup>P. C. Chaumet and M. Nieto-Vesperinas, *Opt. Lett.* **25**, 1065 (2000).
- <sup>16</sup>P. C. Chaumet and M. Nieto-Vesperinas, *Phys. Rev. B* **62**, 11 185 (2000).
- <sup>17</sup>E. M. Purcell and C. R. Pennypacker, *Astrophys. J.* **186**, 705 (1973).
- <sup>18</sup>J. A. Stratton, *Electromagnetic Theory* (McGraw-Hill, New York, 1941).
- <sup>19</sup>J. D. Jackson, *Classical Electrodynamics*, 2nd ed. (John Wiley, New York, 1975), p. 395.
- <sup>20</sup>G. S. Agarwal, *Phys. Rev. A* **11**, 230 (1975); **12**, 1475 (1975).
- <sup>21</sup>A. Rahmani, P. C. Chaumet, and F. de Fornel, *Phys. Rev. A*, **63**, 023819 (2001); A. Rahmani, P. C. Chaumet, F. de Fornel, and C. Girard, *Phys. Rev. A* **56**, 3245 (1997).
- <sup>22</sup>For a small sphere, the gradient and scattering forces are proportional to  $a^3$  and  $a^6$ , respectively.
- <sup>23</sup>L. Cognet, V. Savalli, G. Zs. K. Horvath, D. Holleville, R. Marani, C. I. Westbrook, N. Westbrook, and A. Aspect, *Phys. Rev. Lett.* **81**, 5044 (1998); A. Landragin, J.-Y. Courtois, G. Labeyrie, N. Vansteenkiste, C. I. Westbrook, and A. Aspect, *ibid.* **77**, 1464 (1996).
- <sup>24</sup>K. Okamoto and S. Kawata, *Phys. Rev. Lett.* **83**, 4534 (1999).
- <sup>25</sup>G. L. Klimchitskaya, U. Mohideen, and V. M. Mostepanko, *Phys. Rev. A* **61**, 062107 (2000).
- <sup>26</sup>P. W. Milonni, *Phys. Rev. A* **53**, 3484 (1996).